Published in final edited form as:
Anal Biochem. 2009 March 1; 386(1): 91–97. doi:10.1016/j.ab.2008.11.036.

A fluorescence resonance energy transfer-based approach for investigating late endosome–lysosome retrograde fusion events

A.M. Kaufmann, **S.D.B. Goldman**, and **J.P. Krise***
Department of Pharmaceutical Chemistry, University of Kansas, 2095 Constant Ave., Lawrence, KS 66047, USA

Abstract

Traditionally, lysosomes have been considered to be a terminal endocytic compartment. Recent studies suggest that lysosomes are quite dynamic, being able to fuse with other late endocytic compartments as well as with the plasma membrane. Here we describe a quantitative fluorescence energy transfer (FRET)-based method for assessing rates of retrograde fusion between terminal lysosomes and late endosomes in living cells. Late endosomes were specifically labeled with 800-nm latex beads that were conjugated with streptavidin and Alexa Fluor 555 (FRET donor). Terminal lysosomes were specifically labeled with 10,000-MW dextran polymers conjugated with biotin and Alexa Fluor 647 (FRET acceptor). Following late endosome–lysosome fusion, the strong binding affinity between streptavidin and biotin brought the donor and acceptor fluorophore molecules into close proximity, thereby facilitating the appearance of a FRET emission signal. Because apparent size restrictions in the endocytic pathway do not permit endocytosed latex beads from reaching terminal lysosomes in an anterograde fashion, the appearance of the FRET signal is consistent with retrograde transport of lysosomal cargo back to late endosomes. We assessed the efficiency of this transport step in fibroblasts affected by different lysosome storage disorders—Niemann–Pick type C, mucolipidosis type IV, and Sandhoff's disease, all of which have a similar lysosomal lipid accumulation phenotype. We report here, for the first time, that these disorders can be distinguished by their rate of transfer of lysosome cargos to late endosomes, and we discuss the implications of these findings for developing new therapeutic strategies.

Keywords

Lysosome; Late endosome; Retrograde fusion; FRET; Traffic

Lysosomes have long been considered as the terminal compartment for fluid phase endocytosis [1]; however, recent findings have shown that lysosomes are able to fuse with prelysosomal compartments, in a retrograde fashion, to result in the formation of so-called hybrid organelles [2,3]. The precise function of such hybrid organelles in cells is not completely understood; however, Griffiths [4] proposed that hybrid organelles may have a digestive role similar to traditional lysosomes.

Jahraus and coworkers [2] were the first to develop a cell-based method that clearly demonstrated the retrograde fusion of terminal lysosomes with prelysosomal compartments. Their method uses a pulse–chase technique specifically localizing sucrose to terminal lysosomes. Because sucrose is not a substrate for lysosomal nutrient transporters, it can accumulate to an extent that causes high osmotic pressure and, therefore, induces the vacuolization of lysosomes. Such vacuoles are referred to as sucrosomes and are clearly visible

*Corresponding author. Fax: +1 785 864 5736. *E-mail address:* E-mail: krise@ku.edu (J.P. Krise).

using conventional light microscopy. Subsequently, cells were incubated with 800-nm latex beads conjugated with the enzyme invertase (sucrase). Latex beads of this size are unique in that they are endocytosed by cells but, by virtue of their size, fail to progress beyond late endosomes to lysosomes [5]. When in the presence of invertase, sucrose is converted into glucose and fructose, both of which are rapidly transported across lysosomal membranes by specific transporter proteins [6]. Transport of these molecules relieves osmotic pressure and results in the shrinking of the sucrosome. Thus, a reduction in sucrosome size is indicative of retrograde fusion of lysosomes with late endosomes. Despite its usefulness in demonstrating retrograde lysosome–late endosome fusion, this method cannot be readily employed to examine rates of hybrid organelle formation.

In this work, we examined whether the concept developed by Jahraus and colleagues [2] could be redesigned to provide a quantitative measure of retrograde lysosome–late endosome fusion. To accomplish this, we investigated the suitability of a fluorescence resonance energy transfer (FRET)[1]-based readout for assessing the extent of these fusion events in living cells. Specifically, we localized 10,000-MW dextran polymers to lysosomes (instead of sucrose) using previously described pulse-chase protocols [7]. The dextran polymer was coupled with biotin and fluorescently labeled with Alexa Fluor 647 (AF647, FRET acceptor). Next, latex beads were localized within late endosomes as described previously [2]. The beads were of the same diameter as used previously by Jahraus and coworkers but were conjugated with streptavidin, instead of invertase, and fluorescently labeled with Alexa Fluor 555 (AF555, FRET donor). If lysosome and late endosome contents mix, the strong binding affinity of streptavidin for biotin should result in the dextran binding to the latex bead. As a result, the fluorescent FRET fluorophores will be in close proximity with each other and result in the appearance of a FRET ratio that is calculated using fluorescence intensities of the donor and acceptor fluorophores [8,9]. By monitoring the appearance of a new FRET ratio over time, we obtain a quantitative readout describing the extent of retrograde traffic originating from the lysosome. To assess FRET probe specificity, probe functionality, and ultimately determination of retrograde lysosome traffic in living cells, a series of controls were performed. The effects of a disrupted microtubule network on the trafficking of lysosome contents, as well as the impact that various lysosome storage disorders (LSDs) have on this retrograde process, were investigated.

Materials and methods

Cell culture

Normal human fibroblasts (cat. no. CRL-2076) were purchased from and cultured according to Coriell Cell Repository (Camden, NJ, USA) instructions. Niemann-Pick type C disease fibroblasts with dysfunctional Niemann-Pick C1 protein (NPC, cat. no. GM-03123), mucolipidosis type IV fibroblasts with dysfunctional mucolipin-1 protein (MLIV, cat. no. GM-02408), and Sandhoff's disease fibroblasts with defective hexosaminidase activity (cat. no. GM-11707) were purchased from and cultured according to American Type Culture Collection (ATCC, Manassas, VA, USA) instructions. Cells were cultured in Corning cell culture flasks at 37 °C in a 5% CO_2 humidified atmosphere until monolayers were 80% confluent, at which time they were subcultured or seeded for experimentation. All experiments were performed with cells before the fifth subculture. For live cell experiments, a TC-MI

[1]*Abbreviations used:* FRET, fluorescence resonance energy transfer; AF647, Alexa Fluor 647; AF555, Alexa Fluor 555; LSD, lysosome storage disorder; NPC, Niemann–Pick type C disease fibroblasts with dysfunctional Niemann–Pick C1 protein; MLIV, mucolipidosis type IV fibroblasts with dysfunctional mucolipin-1 protein; BDA-10000, biotinylated dextran–amine, 10,000 MW; SE, succinimidyl ester; DMSO, dimethyl sulfoxide; EDAC, *N*-(3-dimethylaminopropyl)-*N′*-ethylcarbodiimide; PBS, phosphate-buffered saline; BSA, bovine serum albumin; LAMP1, lysosome-associated membrane protein-1; CI-MPR, cation-independent mannose-6-phosphate receptor; EEA1, early endosome antigen-1; HRP, horseradish peroxidase; DMEM, Dulbecco's modified Eagle's medium; NOC, nocodazole; PMT, photomultiplier tube; PNS, postnuclear supernatant; NPC1, Niemann–Pick C1; ASF, asialofetuin; IgA, immuno-globulin A.

temperature-controlled humidified chamber from Bioscience Tools (San Diego, CA, USA) was used for the duration of the experiment.

Late endosome and lysosome probe construction

To construct the fluorescent FRET donor and acceptor probes, standard labeling strategies were employed. For the lysosome probe, biotinylated dextran-amine (BDA-10000, 10,000 MW) was fluorescently labeled with the amine-reactive succinimidyl ester (SE) derivative of AF647 per Invitrogen's (Carlsbad, CA, USA) instructions. First, the AF647-SE was reconstituted in dry dimethyl sulfoxide (DMSO) to a concentration of 10 mg/ml. BDA-10000 was reconstituted to 50 mg/ml in 0.1 M sodium bicarbonate buffer (pH 9.0, buffer A), of which a 100-μl aliquot was added to 75 μl of buffer A and 25 μl of 10 mg/ml AF647-SE stock solution. The reaction was carried out at room temperature for 2 h and was quenched with Tris. The resulting solution was desalted five times using protein desalting columns from Thermo Scientific (Rockford, IL, USA) to remove unconjugated AF647. For the late endosome probe, carboxylate-modified monodisperse polystyrene beads (2.5% solids, 1.08×10^{11} beads/ml, 0.792 ± 0.037 μm) were used. First, the beads were activated using *N*-(3-dimethylaminopropyl)-*N′*-ethylcarbodiimide (EDAC). To accomplish this, 4 ml of the polystyrene beads was washed three times with 0.1 M Mes buffer (pH 6.0, buffer B) by centrifuging the beads at 5000g for 20 min and resuspending with buffer B. Immediately after the final wash, the beads were resuspended to a 2% solids mixture in buffer B and 2 ml of freshly prepared 50 mg/ml EDAC was added dropwise to the suspension. The EDAC was allowed to activate the carboxylate groups for 15 min at room temperature, followed by three washes with 0.1 M phosphate-buffered saline (PBS, pH 7.4, buffer C). Activated beads were then resuspended in 5 ml of buffer C for subsequent streptavidin conjugation. Lyophilized streptavidin (Invitrogen) was reconstituted in buffer C at a concentration of 1 mg/ml, of which 5 ml was added to the activated beads solution for 3 h at room temperature. Unconjugated streptavidin was removed by extensive washing with PBS. The beads were centrifuged and stored at 4 °C in a solution of buffer C containing 0.1% glycine to mask any unreacted sites. Fluorescence labeling of the streptavidin-conjugated beads was carried out using the SE derivative of AF555 per Invitrogen's instructions. First, 1 ml of streptavidin-conjugated beads was washed two times with buffer A to remove the glycine storage buffer and then resuspended back to 1 ml. An AF555-SE aliquot of 10 μl was added to the freshly washed beads. Labeling was performed at room temperature for 2 h and subsequently quenched with Tris. Free AF555-SE was removed with extensive washing with PBS. Subsequent dialysis was performed against PBS using a 3.5-kDa cutoff dialysis cassette. Beads were centrifuged once more, resuspended in PBS, and stored at 4 °C until needed. As a control, bovine serum albumin (BSA) was conjugated to latex beads and fluorescently labeled using the same procedures as with streptavidin.

Fluorescence microscopy

Fluorescence micrographs were acquired using a Nikon Eclipse 80i fluorescence microscope with a Hamamatsu Orca ER camera and MetaMorph (version 7.0) software. Filter sets specific for rho-damine and Cy5 (Chroma, Rockingham, VT, USA) were used to detect AF555 and AF647 fluorescence emissions ($AF555_{em}$ and $AF647_{em}$), respectively. Microscope settings were kept identical for the duration of experiments. Immunofluorescence was accomplished using procedures described previously by our laboratory [10].

Lysosome isolation and Western blot analysis

Lysosomes were isolated using previously described methods with modifications to allow isolations in adherent cells. Subsequent Western blot analysis was performed using procedures described previously [7]. Primary antibodies were LAMP1 (lysosome-associated membrane protein-1, 1:500) and CI-MPR (cation-independent mannose-6-phosphate receptor, 1:50) from

Developmental Studies Hybridoma (University of Iowa) and EEA1 (early endosome antigen-1, 1:250) and Golgin-84 (1:250) from BD Biosciences (San Jose, CA, USA). Secondary horseradish peroxidase (HRP)-conjugated antibodies were diluted 1:1000.

Probe localization and treatments

Cells were seeded in 8-well culture chambers at 75,000 cells per well and allowed to adhere overnight. Cells were then incubated for 2 h with 2.5 mg/ml AF647 biotinylated dextran in complete medium, washed once with PBS, and given chase in complete phenol red-free Dulbecco's modified Eagle's medium (DMEM) for 20 h to ensure localization into the lysosome. After 20 h postchase, cells were exposed to 1.28×10^7 beads/ml AF555 streptavidin-conjugated latex beads for 2 h and chased for 1 h to label the late endosomal compartment as described previously [2]. Nocodazole (NOC) administration was accomplished by replacing cell culture medium with complete medium containing 50 μM NOC 1 h after the start of fluorescence intensity measurements.

Fluorescence intensity acquisition and analysis

Fibroblasts were analyzed using a Photon Technologies International (Birmingham, NJ, USA) RatioMaster microscope-mounted spectrofluorimeter with photomultiplier tube (PMT) detection and Felix 32 software. All dichroic and emission filters were obtained from Chroma.

For each time point, three fluorescence intensity measurements were made to calculate the FRET ratio (see below). These fluorescence intensities correspond to the donor excitation/emission ($AF555_{em}$, excitation 550 nm, emission 610/40 nm, dichroic 565 nm longpass), donor excitation/acceptor emission ($FRET_{em}$, excitation 550 nm, emission 710/60 nm, dichroic 565 nm longpass), and acceptor excitation/emission ($AF647_{em}$, excitation 650 nm, emission 670/40 nm, dichroic 660 longpass). To correct for both spectral cross-talk of the fluorescent FRET probes (detection of donor fluorescence with the acceptor emission filter or detection of acceptor fluorescence with the donor emission filter) and the propensity of cell populations to endocytose differential amounts of the probes, we applied a widely used equation for the normalization of observed FRET emission ($FRET_{em}$) intensities to the donor and acceptor emission intensities ($AF555_{em}$ and $AF647_{em}$) present in each set of cells (Eq. (1)) [9,11–13]. Correction factors α and β for cross-talk of the fluorophores into the $FRET_{em}$ filters (see above) were determined to be 0.011 and 0.799, respectively, for our experimental setup. These values were determined by observing cells incubated with only AF555 streptavidin beads or AF647 biotinylated dextran and subsequently measuring their respective contributions to the $FRET_{em}$ measurement. For example, observed $FRET_{em}$ intensities consisted of 1.1% of $AF555_{em}$ and 79.9% of total $AF647_{em}$ signal bleeding into the $FRET_{em}$ filter setup.

$$\text{FRET ratio} = \frac{\text{FRET}_{em} - \alpha \times \text{AF555}_{em} - \beta \times \text{AF647}_{em}}{\sqrt{\text{AF555}_{em} \times \text{AF647}_{em}}}. \quad (1)$$

For each experiment, initial (t = 0 h) FRET ratio values were calculated and normalized to zero, and the appearance of the new FRET ratio signal was evaluated over time. Each fluorescence intensity acquisition was no longer than 10 s.

There are many contributing factors that can result in FRET ratio artifacts in living cells, including cellular autofluorescence [14,15], spectral cross-talk, and differential concentrations of the donor and acceptor present [9,11,15]. To account for autofluorescence from our experimental conditions, we measured fluorescence emission intensities of cells without probes, at wavelength intervals corresponding to each of the probes, in the presence of phenol red-free DMEM containing fetal bovine serum. Although no significant emission peaks were

observed around wavelengths used to measure $AF555_{em}$ and $AF647_{em}$, there was significant background that contributed to the probes' apparent signal (see Fig. S2 in supplementary material). These scans, without probes, were subsequently subtracted from experimental fluorescence intensities before calculating the FRET ratio (see Eq. (1)).

Probe functionality

To assess functionality of the constructed probes, omission control experiments were performed. Confirmation of probe binding was accomplished in vitro by adding 1.28×10^7 beads/ml of AF555 streptavidin-conjugated latex beads to a solution containing 1 mg/ml of either AF647 biotinylated dextran or Alexa Fluor 488 dextran without biotin. The mixture was incubated for 3 h at room temperature, centrifuged, and washed with PBS four times. Aliquots were then analyzed by fluorescence microscopy as described below.

Determination of intracellular FRET efficiency (E) was accomplished using the donor AF555 streptavidin latex bead emission intensities in the presence ($AF555_{both}$) and absence ($AF555_{only}$) of acceptor AF647 biotinylated dextran per Eq. (2) [16]. Using this equation, FRET efficiency was found to be 48.1% when probes interacted in living cells. Competition of AF647 biotinylated dextran from the latex beads was accomplished by adding 0.1 mM (10× excess) of free biotin to the incubation medium for 3 h after the initial FRET probe interaction.

$$E = 1 - (AF555_{both} / AF555_{only}). \quad (2)$$

To establish pH effects on the probe fluorescence intensities, emission intensities ($AF555_{em}$ and $AF647_{em}$) of the fully conjugated probes were measured separately in buffers of different pH levels at a constant ionic strength. The concentration of probes was 0.1 mg/ml AF647 biotinylated dextran and 2.13×10^6 beads/ml for AF555 streptavidin beads.

Results

Synthesis and characterization of FRET probes

Based on previously described methods for specifically localizing probes to lysosomes and late endosomes [2], modified organelle probes were constructed and conjugated with either streptavidin or biotin and a fluorophore that could be used for FRET studies. For lysosomes, we used a commercially available 10,000-MW dextran polymer that was conjugated with both biotin and lysine groups. For late endosomes, we conjugated carboxylate-modified latex beads, of the same diameter (0.792 μm) used by Jahraus and coworkers [2], with streptavidin. Fluorescence labeling of the probes was accomplished by using amine-reactive SE derivatives of the known FRET pair fluorophores AF555 (donor) and AF647 (acceptor) against lysine residues present on streptavidin and dextran, respectively. To confirm specific binding of the biotinylated dextran with streptavidin-coated beads in vitro, both probes were mixed, washed extensively, and imaged. The addition of biotinylated dextran to a solution of streptavidin beads resulted in the appearance of dextran on the perimeter of the beads (Fig. 1A). Binding of the probes allows the FRET fluorophores to come into close proximity to each other, as is required for efficient FRET to occur [8]. Alexa Fluor 488 dextran, without biotin, was used as a negative control and did not bind to the streptavidin beads under the same conditions (Fig. 1A).

For efficient FRET to occur, the FRET fluorophores are required to be in close proximity so that donor fluorescence intensity is quenched by the presence of an acceptor [8]. Streptavidin and biotin facilitate this spatial requirement when bound together and have been used in previous FRET evaluations [17]. To establish the functionality of our constructed FRET probes, we performed a series of controls to evaluate FRET efficiency in living cells. If the spatial requirements of FRET are met through the binding of biotin to streptavidin, then latex

bead conjugation to a protein with less affinity for biotin should result in decreased quenching of the donor fluorophore emission. Thus, we constructed new beads conjugated with BSA, which was also tagged with AF555, to evaluate whether nonspecific associations between the probes could cause donor quenching. In the absence of AF647 biotinylated dextran, we observed that beads coated with streptavidin had a higher relative fluorescence signal when excited at the donor excitation of 550 nm than did BSA-coated beads (Fig. 1B). In the presence of AF647 biotinylated dextran, streptavidin-coated beads had a lower fluorescence signal than did BSA beads. This decrease occurs from the donor emission intensity being efficiently quenched by the presence of an acceptor fluorophore and was not observed with BSA-conjugated beads. To rescue AF555 streptavidin bead fluorescence, we performed a biotin competition experiment and found that the donor emission was no longer quenched (Fig. 1B). This was due to the displacement of AF647 biotinylated dextran from AF555 streptavidin by the nonfluorescent biotin, resulting in distances not conducive to efficient FRET.

Hoppe and coworkers reported that pH-dependent fluorescence intensity fluctuations of FRET fluorophores can result in decreased FRET efficiency between donor and acceptor molecules [12]. To be certain that our fluorescent probes were suitable for studies in which pH could be manipulated, whether from endogenous factors or from exogenously supplied agents, we characterized fluorescence intensities over a broad pH range. We found that fluorescence intensities remained constant for each probe and did not fluctuate significantly at pH values relevant to the endocytic pathway (Fig. 1C).

Intracellular localization of the FRET probes

To examine the suitability of our pulse–chase protocols, we examined the localization of both fluorescent probes in normal human fibroblasts used in this work. To accomplish this, subcellular organelle isolations and immunofluorescence microscopy were performed after the probes were endocytosed as described in Materials and Methods. For immunofluorescence, cells were fixed and probed with antibodies specific to the LAMP1 for lysosomes and the CI-MPR for late endosomes. The majority of the biotinylated dextran was found in LAMP1-positive, CI-MPR-negative organelles (see Fig. S1 in supplementary material) indicative of the lysosome [18]. For lysosome isolations, a super-paramagnetic iron dextran was localized to lysosomes using the same incubation conditions as the biotinylated dextran. Lysosomes were then purified using a magnetic chromatography approach developed in our laboratory [7]. Western blot analysis revealed the presence of CI-MPR in the postnuclear supernatant (PNS) but not in the isolated fraction (Fig. 2A). Furthermore, there was no significant localization into either the Golgi apparatus (Golgin-84) or early endosomes (EEA1), suggesting that the biotinylated dextran is almost completely in lysosomes when using optimized pulse–chase conditions (Fig. 2B). Immunofluorescence of cells incubated with streptavidin beads shows localization within CI-MPR-positive organelles, indicating that the beads were predominantly in late endosomes (Fig. 2C).

Interactions of FRET probes occur in vivo

Earlier, we showed that the fluorescent FRET probes could bind in vitro (Fig. 1A). Considering that the lumenal composition of late endosomes and lysosomes is much more complex than PBS, we evaluated whether the FRET probes could interact and colocalize to a significant degree in vivo. To accomplish this, dextran was endocytosed as before and cells were visualized using fluorescence microscopy at the end of the streptavidin bead chase (0 h) and 24 h postchase. Initially, the two probes were visualized in separate compartments. However, at 24 h postchase, dextran signal was observed in bead-containing compartments, suggesting that a significant portion of lysosomal dextran was bound to the streptavidin beads (Fig. 3).

Retrograde transport of lysosome cargo to late endosomes is microtubule dependent

The movements of lysosomes and late endosomes have been shown to be microtubule dependent [19]. The addition of a reagent that destabilizes microtubules, inhibiting the contact between lysosomes and late endosomes, should diminish retrograde lysosome traffic and, thus, decrease the FRET ratio over time. To test this, the microtubule-destabilizing agent NOC was incubated with cells. First, lysosomes and late endosomes were allowed to interact for 1 h, at which point cells were either treated with 50 μM NOC or left untreated. By not pretreating cells with NOC prior to fluorescence intensity measurements, we created the same initial conditions with respect to probe uptake given that NOC would affect microtubule-dependent endocytosis of the latex beads. Furthermore, allowing lysosomes and late endosomes to interact for 1 h allowed us to evaluate the postadministration effects of NOC in real time. After NOC treatment, the appearance of the new FRET ratio was minimal compared with that of normal untreated cells (Fig. 4). This indicated that NOC destabilization of the microtubule network impacted organelle interactions and ultimately the ability of biotinylated dextran to be delivered to the late endosome by the retrograde lysosome pathway.

Investigation of retrograde lysosome transport efficiency in LSDs

Many LSDs have been shown to have a hyperaccumulation of sphingolipids and fatty acids in the lysosomes of diseased cells. Examples of these include NPC disease, MLIV, and Sandhoff's disease, which result from defective Niemann–Pick C1 (NPC1), mucolipin-1, and hexosaminidase activities, respectively [20–22]. Despite the inability of affected lysosomes to displace or metabolize these accumulated substrates, the effect of their buildup on vesicular trafficking pathways from the lysosome has not been fully researched. Concurrent with this study, evaluations using the described FRET-based approach illustrated that NPC cells had decreased lysosomal retrograde traffic relative to normal fibroblasts [10]. MLIV and Sandhoff's disease were assayed over a period of 3 h to investigate whether all LSDs possessing lipid buildup phenotypes, similar to NPC disease, had deficient retrograde traffic from their lysosomes (Fig. 5). Interestingly, MLIV and Sandhoff's disease fibroblasts had retrograde lysosome traffic rates nearly identical to those of normal cells. As a control, NPC cells were evaluated and shown to have inefficient retrograde trafficking when compared with normal cells. NPC1 has been shown to be required for the fusion of lysosomes and late endosomes [10]. Results from MLIV and Sandhoff's disease evaluations suggest that functional mucolipin-1 and hexosaminidase are not essential for the retrograde transport of lysosomal cargo to late endosomes. The functionality of certain lysosome proteins such as NPC1, however, is required for this process to occur efficiently. Furthermore, the hyperaccumulation of a variety of lipids within the lysosomal lumen has no effect on the ability of lysosomes to traffic their contents in a retrograde manner to late endosomes, as observed with MLIV and Sandhoff's disease.

Discussion

To date, there have been several different approaches developed to investigate the interactions of lysosomes and late endosomes [2,23,24]. Mullock and coworkers described a cell-free content mixing assay based on the mixing of purified late endosomes and lysosomes harvested from rat livers [24]. Briefly, organelle labeling was accomplished by the endocytosis of avidin–ASF (asialofetuin) to late endosomes and ^{125}I-biotinylated immunoglobulin A (IgA) to lysosomes and was subsequently purified. Each of the fractions was separately reconstituted in cytosol containing an ATP-regenerating system and added together. Evidence of late endosome–lysosome fusion was determined by immunoprecipitation of avidin–ASF that bound to ^{125}I-biotinylated IgA if the two organelles were fused together. Use of this assay has identified many components, such as SNARE, SNAP, and Rab GTPase proteins, which are necessary for fusion of lysosomes with late endosomes [25,26]. Although highly elegant and

informative, such an assay requires lengthy and complex organelle isolation procedures from animals and radioactive reagents. Jahraus and coworkers described a cell-based method for observing retrograde lysosome fusion with late endosomes [2]. Although this method adequately described retrograde lysosome traffic, detection of this event was accomplished qualitatively with light microscopy. This type of analysis would not be suitable for evaluating slight changes in the rates of retrograde traffic that could be useful in identifying the molecular mechanisms underlying this trafficking pathway.

In this article, we have described a method for evaluating lysosome–late endosome fusion that offers a significant advancement over existing methods with regard to assessing retrograde lysosome traffic, specifically that (i) it is amenable to high throughput and (ii) it is quantitative. Using these advancements, the FRET-based approach could allow future studies to further elucidate proteins or other endogenous factors that may influence this retrograde trafficking step. To partially address this possibility, we investigated three different LSDs, all of which present similar phenotypes with regard to sphingolipid and cholesterol accumulation in lysosomes. Interestingly, although the phenotypes are similar, the efficiency of this trafficking pathway can be differentiated between various LSDs. In the case of NPC disease, it is likely that this assay could be used to identify potential small-molecular-weight therapeutic agents that appropriately modulate this trafficking pathway. In support of this, it was recently shown that certain classes of small molecules can either stimulate or inhibit this retrograde trafficking step [10]. Using this FRET-based method, further evaluation of these factors could ultimately provide information to help rationally design therapeutic strategies that can be implemented to alleviate inefficient lysosome egress of cargos in a retrograde fashion.

Supplementary Material

Refer to Web version on PubMed Central for supplementary material.

Acknowledgments

We acknowledge D. Moore and the KU Microscopy and Analytical Imaging facility for technical discussions and the critical reading of this manuscript. All authors participated in the figure preparation and writing of the manuscript. This work was funded by grants from the National Institutes of Health (RO1 CA106655) and the Ara Parseghian Medical Research Foundation to J.P.K.

Appendix A: Supplementary data

Supplementary data associated with this article can be found, in the online version, at doi: 10.1016/j.ab.2008.11.036.

References

1. Mellman I. Endocytosis and molecular sorting. Annu. Rev. Cell Dev. Biol 1996;12:575–625. [PubMed: 8970738]
2. Jahraus A, Storrie B, Griffiths G, Desjardins M. Evidence for retrograde traffic between terminal lysosomes and the prelysosomal/late endosome compartment. J. Cell Sci 1994;107:145–157. [PubMed: 8175904]
3. Bright NA, Reaves BJ, Mullock BM, Luzio JP. Dense core lysosomes can fuse with late endosomes and are re-formed from the resultant hybrid organelles. J. Cell Sci 1997;110:2027–2040. [PubMed: 9378754]
4. Griffiths G. On vesicles and membrane compartments. Protoplasma 1996;195:37–58.
5. Rabinowitz S, Horstmann H, Gordon S, Griffiths G. Immunocytochemical characterization of the endocytic and phagolysosomal compartments in peritoneal macrophages. J. Cell Biol 1992;116:95–112. [PubMed: 1730752]

6. Mancini GM, Beerens CE, Verheijen FW. Glucose transport in lysosomal membrane vesicles: kinetic demonstration of a carrier for neutral hexoses. J. Biol. Chem 1990;265:12380–12387. [PubMed: 2373697]
7. Duvvuri M, Krise JP. A novel assay reveals that weakly basic model compounds concentrate in lysosomes to an extent greater than pH-partitioning theory would predict. Mol. Pharmacol 2005;2:440–448.
8. Lakowicz, JR. New York: Kluwer Academic/Plenum; 1999. Principles of Fluorescence Spectroscopy.
9. Xia Z, Liu Y. Reliable and global measurement of fluorescence resonance energy transfer using fluorescence microscopes. Biophys. J 2001;81:2395–2402. [PubMed: 11566809]
10. Kaufmann AM, Krise JP. Niemann–Pick C1 functions in regulating lysosomal amine content. J. Biol. Chem 2008;283:24584–24593. [PubMed: 18591242]
11. Gordon GW, Berry G, Liang XH, Levine B, Herman B. Quantitative fluorescence resonance energy transfer measurements using fluorescence microscopy. Biophys. J 1998;74:2702–2713. [PubMed: 9591694]
12. Hoppe A, Christensen K, Swanson JA. Fluorescence resonance energy transfer-based stoichiometry in living cells. Biophys. J 2002;83:3652–3664. [PubMed: 12496132]
13. Hillebrand M, Verrier SE, Ohlenbusch A, Schafer A, Soling HD, Wouters FS, Gartner J. Live cell FRET microscopy: homo- and heterodimerization of two human peroxisomal ABC transporters, the adrenoleukodystrophy protein (ALDP, ABCD1) and PMP70 (ABCD3). J. Biol. Chem 2007;282:26997–27005. [PubMed: 17609205]
14. Aubin JE. Autofluorescence of viable cultured mammalian cells. J. Histochem. Cytochem 1979;27:36–43. [PubMed: 220325]
15. Sebestyen Z, Nagy P, Horvath G, Vamosi G, Debets R, Gratama JW, Alexander DR, Szollosi J. Long wavelength fluorophores and cell-by-cell correction for autofluorescence significantly improves the accuracy of flow cytometric energy transfer measurements on a dual-laser benchtop flow cytometer. Cytometry 2002;48:124–135. [PubMed: 12116358]
16. Turcatti G, Nemeth K, Edgerton MD, Meseth U, Talabot F, Peitsch M, Knowles J, Vogel H, Chollet A. Probing the structure and function of the tachykinin neurokinin-2 receptor through biosynthetic incorporation of fluorescent amino acids at specific sites. J. Biol. Chem 1996;271:19991–19998. [PubMed: 8702716]
17. Nikiforov TT, Beechem JM. Development of homogeneous binding assays based on fluorescence resonance energy transfer between quantum dots and Alexa Fluor fluorophores. Anal. Biochem 2006;357:68–76. [PubMed: 16860286]
18. Dintzis SM, Velculescu VE, Pfeffer SR. Receptor extracellular domains may contain trafficking information: studies of the 300-kDa mannose 6-phosphate receptor. J. Biol. Chem 1994;269:12159–12166. [PubMed: 8163521]
19. Deng YP, Storrie B. Animal cell lysosomes rapidly exchange membrane proteins. Proc. Natl. Acad. Sci. USA 1988;85:3860–3864. [PubMed: 3287378]
20. Chen CS, Bach G, Pagano RE. Abnormal transport along the lysosomal pathway in mucolipidosis, type IV disease. Proc. Natl. Acad. Sci. USA 1998;95:6373–6378. [PubMed: 9600972]
21. Bolhuis PA, Oonk JG, Kamp PE, Ris AJ, Michalski JC, Overdijk B, Reuser AJ. Ganglioside storage, hexosaminidase lability, and urinary oligosaccharides in adult Sandhoff's disease. Neurology 1987;37:75–81. [PubMed: 2948136]
22. Kruth HS, Comly ME, Butler JD, Vanier MT, Fink JK, Wenger DA, Patel S, Pentchev PG. Type C Niemann–Pick disease: abnormal metabolism of low density lipoprotein in homozygous and heterozygous fibroblasts. J. Biol. Chem 1986;261:16769–16774. [PubMed: 3782141]
23. Bright NA, Gratian MJ, Luzio JP. Endocytic delivery to lysosomes mediated by concurrent fusion and kissing events in living cells. Curr. Biol 2005;15:360–365. [PubMed: 15723798]
24. Mullock BM, Perez JH, Kuwana T, Gray SR, Luzio JP. Lysosomes can fuse with a late endosomal compartment in a cell-free system from rat liver. J. Cell Biol 1994;126:1173–1182. [PubMed: 7520447]
25. Mullock BM, Bright NA, Fearon CW, Gray SR, Luzio JP. Fusion of lysosomes with late endosomes produces a hybrid organelle of intermediate density and is NSF dependent. J. Cell Biol 1998;140:591–601. [PubMed: 9456319]

26. Mullock BM, Smith CW, Ihrke G, Bright NA, Lindsay M, Parkinson EJ, Brooks DA, Parton RG, James DE, Luzio JP, Piper RC. Syntaxin 7 is localized to late endosome compartments, associates with Vamp 8, and is required for late endosome–lysosome fusion. Mol. Biol. Cell 2000;11:3137–3153. [PubMed: 10982406]

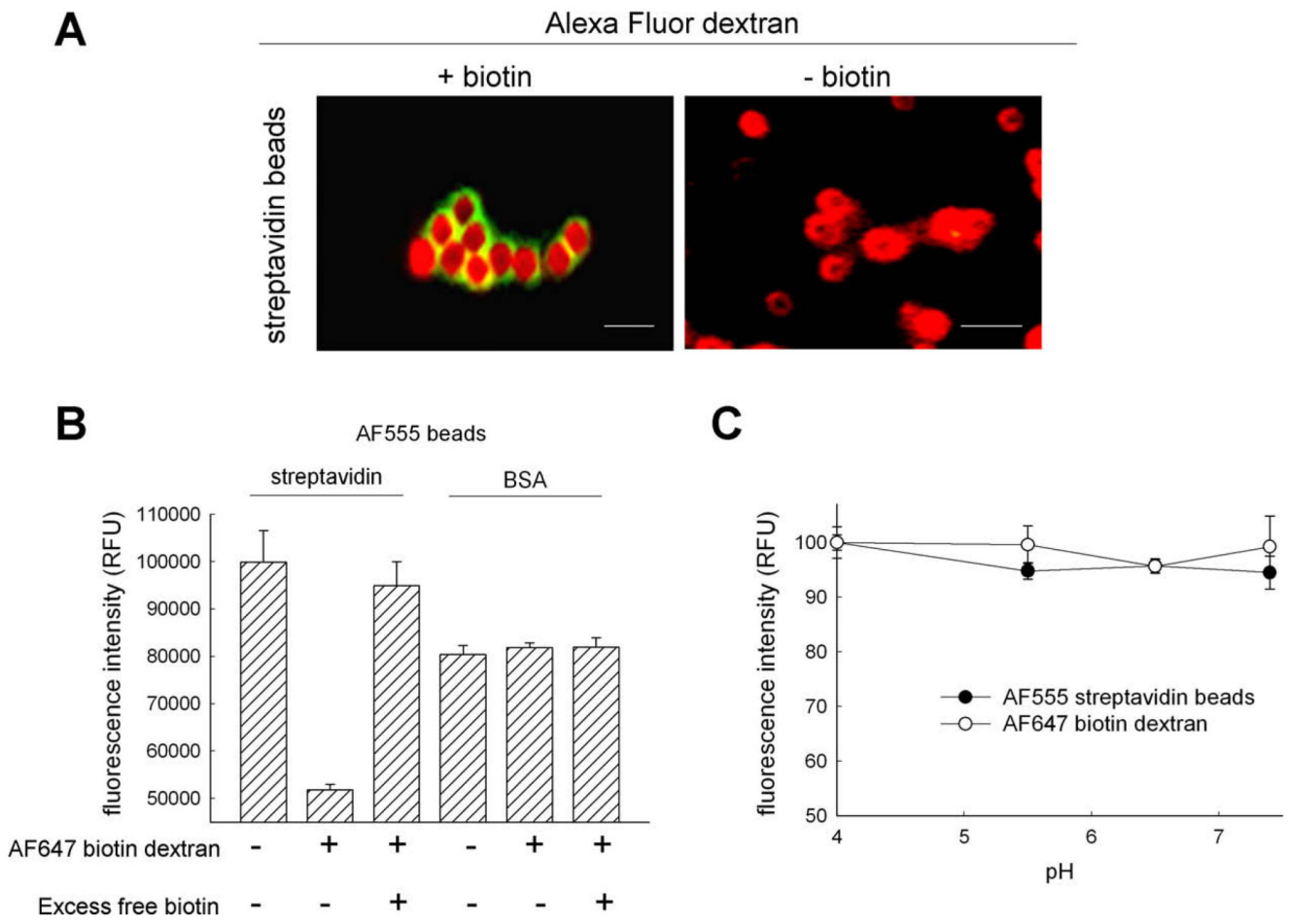

Fig. 1.

Functional characterization of FRET-based organelle probes. Fluorescent organelle-specific probes with FRET properties were constructed using modified previously described methods [2]. (A) Fully conjugated probes were incubated together and imaged. Binding of dextran (green) to streptavidin latex beads (red) was dependent on the presence of biotin on the dextran polymer. Scale bar represents 1 μm. (B) FRET efficiency determination by fluorescence quenching of the donor FRET probe AF555. Raw fluorescence intensities of AF555-labeled streptavidin or BSA-conjugated beads were measured in the presence and absence of AF647 biotinylated dextran. Significant quenching of AF555 emission occurs when streptavidin is conjugated to the latex beads and can be rescued by incubating with excess biotin to remove AF647 biotinylated dextran. Fluorescence intensities for BSA-conjugated beads remained constant in the presence and absence of AF647 biotinylated dextran or excess biotin. (C) Fluorescence intensities of FRET probes as a function of pH. AF647-labeled biotinylated dextran (●) and AF555-labeled streptavidin beads (○) were incubated in buffers of different pH levels, and their fluorescence intensities were measured. No significant change in intensities of either probe was observed at lower pH levels. (For interpretation of the references to color in this figure legend, the reader is referred to the Web version of this article.)

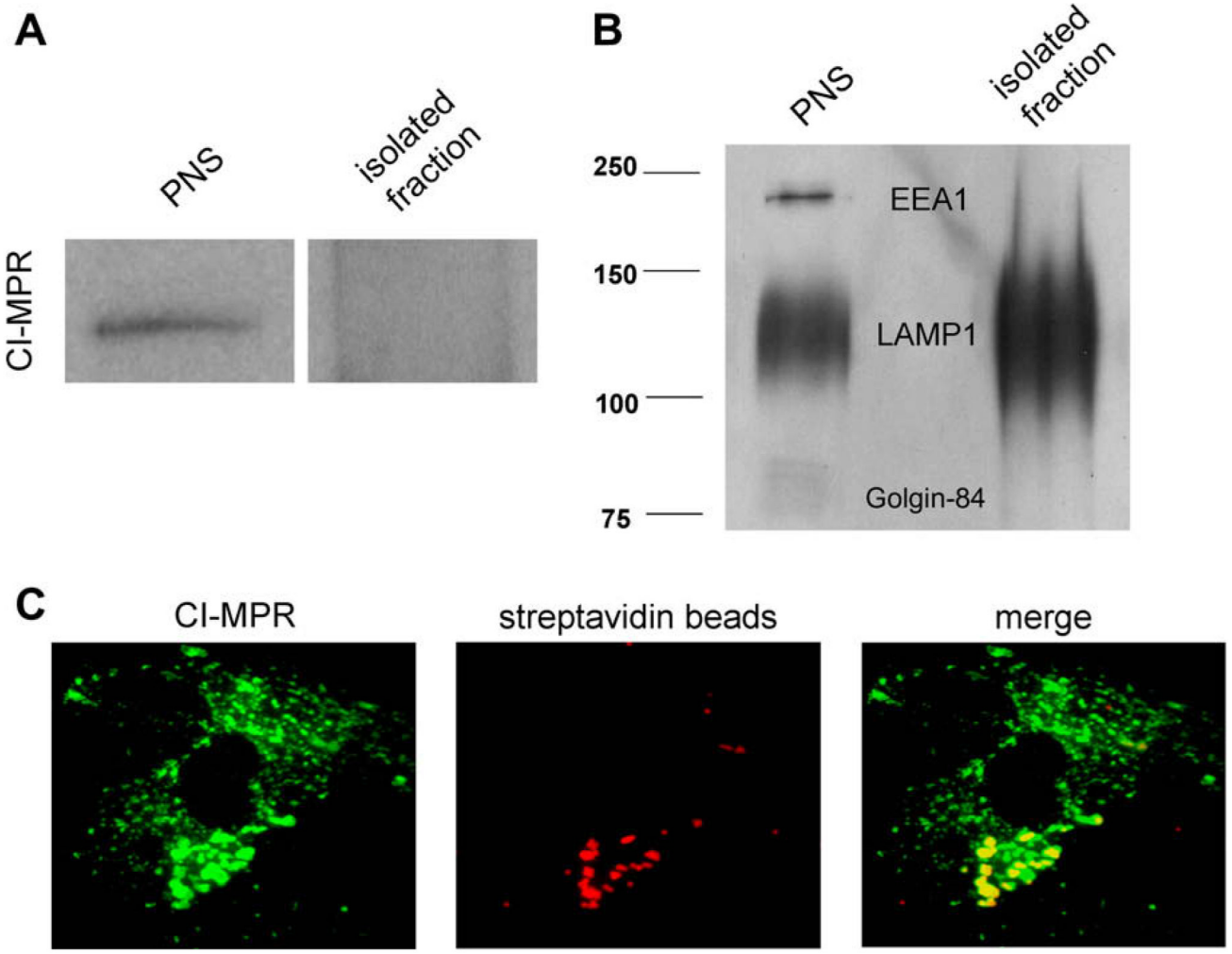

Fig. 2.

Western blot and immunofluorescence analysis shows intracellular localization of the FRET probes in two biochemically distinct compartments. Using optimized pulse–chase conditions, FRET probes were endocytosed into cells and their specific organelle localization was analyzed. (A) Magnetic isolation of lysosomes using iron-coated dextran of the same size was performed as described previously [7]. Western blot analysis was performed using antibodies specific to the CI-MPR. (B) Golgin-84, EEA1, and LAMP1 on fractions of PNS and isolated lysosomes. The isolated lysosome fraction was found to be devoid of late endosome, early endosome, and Golgi protein markers and enriched in LAMP1. (C) Immunofluorescence was performed after endocytosis of streptavidin beads (red). The beads were found to localize in CI-MPR-positive (green) compartments. (For interpretation of the references to color in this figure legend, the reader is referred to the Web version of this article.)

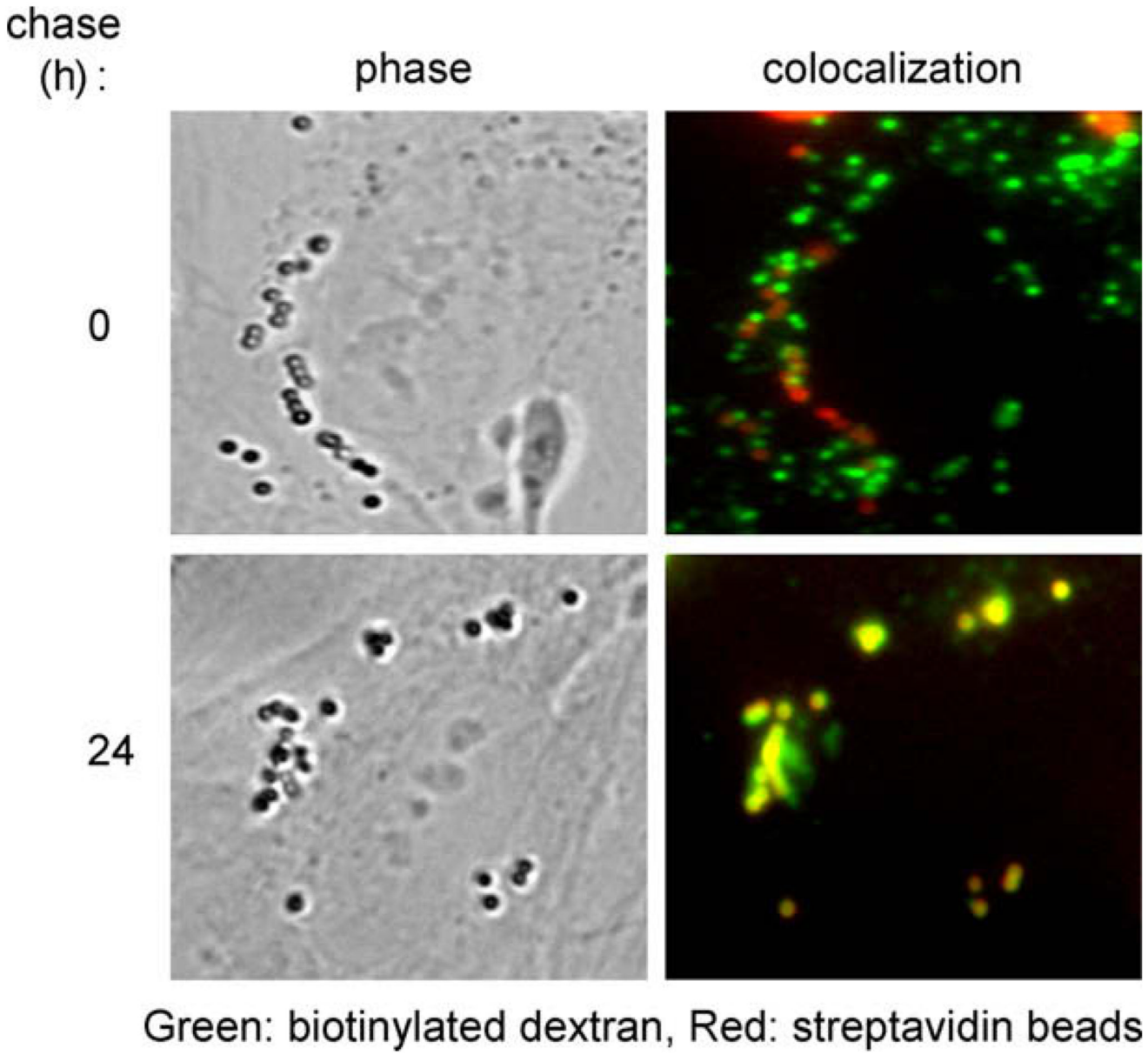

Fig. 3.

Fluorescence microscopy reveals that FRET probes interact and colocalize intracellularly in normal fibroblasts. Intracellular interactions were observed between the organelle-specific probes after sufficient chase. Initially, the probes were not significantly colocalized with each other. However, after a 24-h chase, the AF647 biotinylated dextran (green) was found bound to the AF555 streptavidin beads (red) in living cells. (For interpretation of the references to color in this figure legend, the reader is referred to the Web version of this article.)

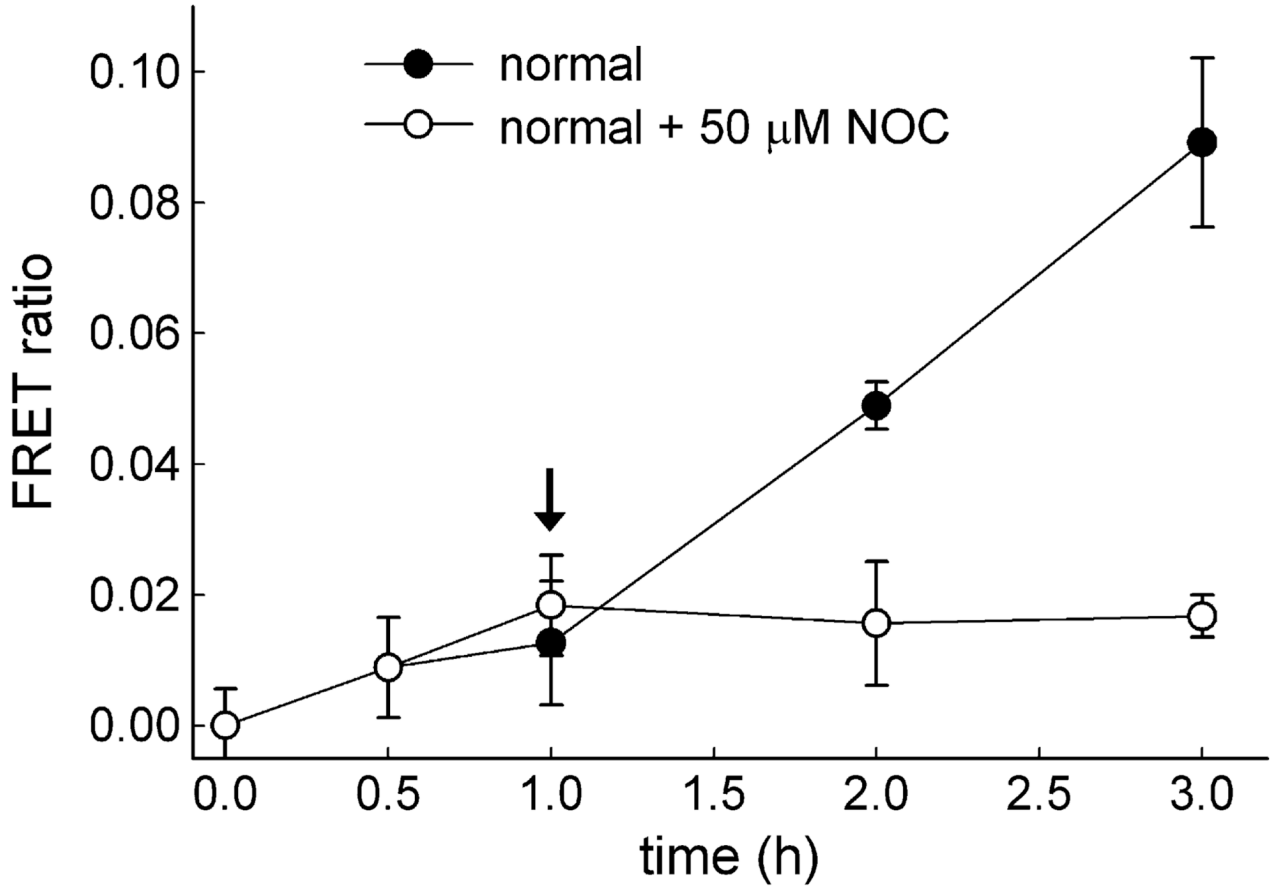

Fig. 4.

FRET ratio profile illustrating that retrograde lysosome fusion with late endosomes requires an intact microtubule network. Calculated FRET ratio values were determined at each time point for cells treated (○) and left untreated (●) with the microtubule depolymerizing agent NOC 1 h into the experiment (arrow). NOC treatment resulted in a diminished FRET ratio over time, indicating a negative impact on retrograde lysosome traffic. Results are averages of three independent experiments ± standard deviations.

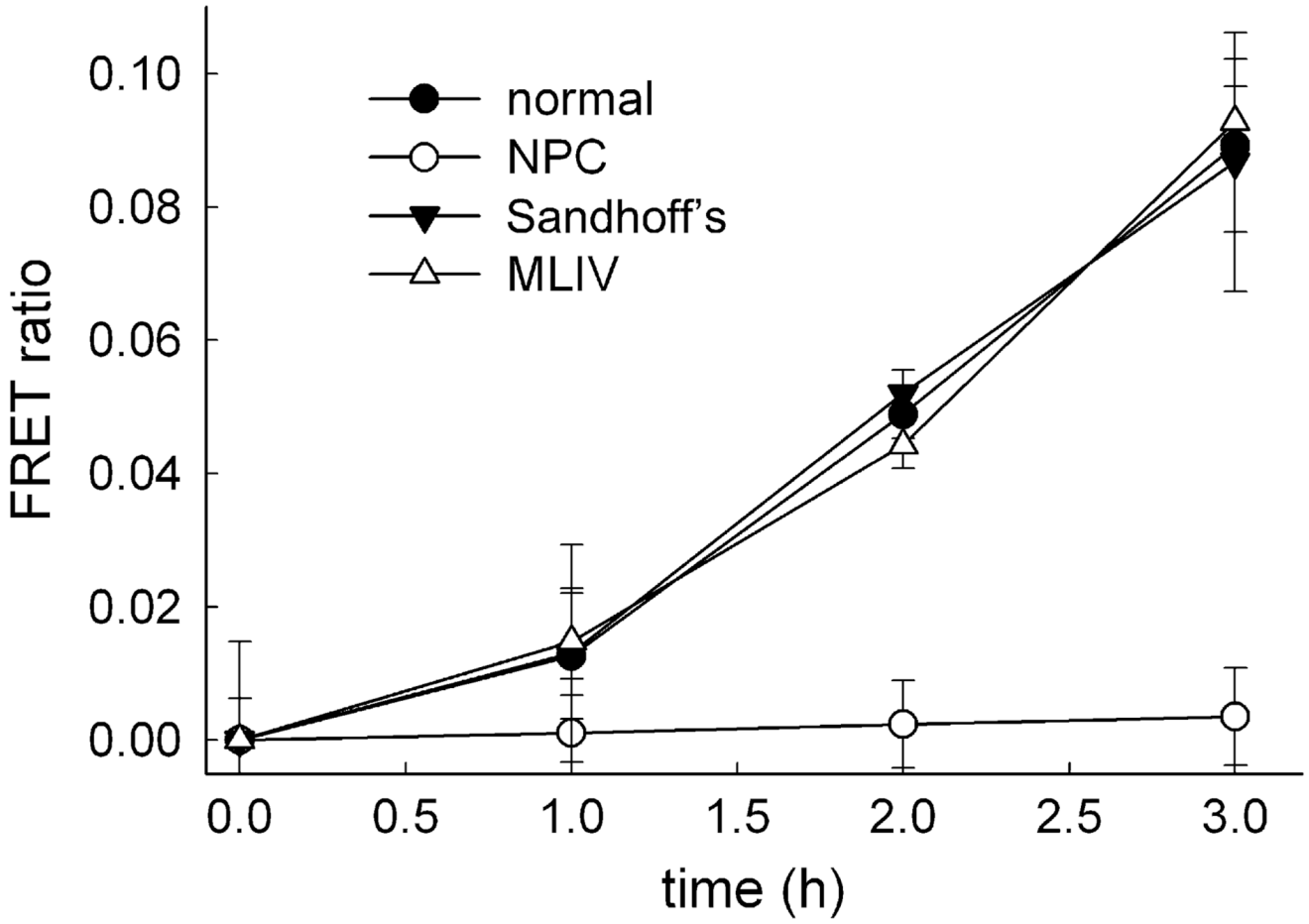

Fig. 5.

Lysosomal storage disorders have different retrograde lysosome fusion rates with late endosomes. Calculated FRET ratio values for each time point were determined for normal cells and for cells with LSDs–NPC, MLIV, and Sandhoff's disease. Lysosomes of NPC-affected cells have inefficient retrograde transport of contents given that they lack the appearance of FRET ratio over time when compared with MLIV and Sandhoff's disease fibroblasts, which exhibit rates similar to those of normal cells. Results are averages of three independent experiments ± standard deviations.